Biochimica et Biophysica Acta 1833 (2013) 2057–2069

Contents lists available at SciVerse ScienceDirect

Biochimica et Biophysica Acta

journal homepage: www.elsevier.com/locate/bbamcr

Salinomycin induces activation of autophagy, mitophagy and affects mitochondrial polarity: Differences between primary and cancer cells

Jaganmohan Reddy Jangamreddy [a,b], Saeid Ghavami [c,d], Jerzy Grabarek [e], Gunnar Kratz [b,f,g], Emilia Wiechec [a,b], Bengt-Arne Fredriksson [h], Rama Krishna Rao Pariti [a,b], Artur Cieślar-Pobuda [a,b,i], Soumya Panigrahi [j], Marek J. Łos [a,b,e,*]

[a] Depart. Clinical and Experimental Medicine (IKE), Division of Cell Biology, Linköping Univ., Sweden
[b] Integrative Regenerative Medicine Center (IGEN), Linköping University, Sweden
[c] Department of Physiology, Univ. Manitoba, Winnipeg, Canada
[d] Manitoba Institute of Child Health, Univ. Manitoba, Winnipeg, Canada
[e] Department of Pathology, Pomeranian Medical University, Szczecin, Poland
[f] Experimental Plastic Surgery, IKE, Linköping University, Sweden
[g] Department of Plastic Surgery, County of Östergötland, Linköping, Sweden
[h] Microscopy Unit, Core Facility, Faculty of Health Sciences, Linköping University, Sweden
[i] Biosystems Group, Institute of Automatic Control, Silesian University of Technology, Gliwice, Poland
[j] Department of Molecular Cardiology, Lerner Research Institute/NB-50, 9500 Euclid Avenue, Cleveland, OH 44195, USA

ARTICLE INFO

Article history:
Received 22 March 2013
Received in revised form 16 April 2013
Accepted 21 April 2013
Available online 29 April 2013

Keywords:
Cancer stem cells
Mitofusin
Mitophagy
mTOR
PGC1α
Salinomycin

ABSTRACT

The molecular mechanism of Salinomycin's toxicity is not fully understood. Various studies reported that Ca^{2+}, cytochrome c, and caspase activation play a role in Salinomycin-induced cytotoxicity. Furthermore, Salinomycin may target Wnt/β-catenin signaling pathway to promote differentiation and thus elimination of cancer stem cells. In this study, we show a massive autophagic response to Salinomycin (substantially stronger than to commonly used autophagic inducer Rapamycin) in prostrate-, breast cancer cells, and to lesser degree in human normal dermal fibroblasts. Interestingly, autophagy induced by Salinomycin is a cell protective mechanism in all tested cancer cell lines. Furthermore, Salinomycin induces mitophagy, mitoptosis and increased mitochondrial membrane potential ($\Delta\Psi$) in a subpopulation of cells. Salinomycin strongly, and in time-dependent manner decreases cellular ATP level. Contrastingly, human normal dermal fibroblasts treated with Salinomycin show some initial decrease in mitochondrial mass, however they are largely resistant to Salinomycin-triggered ATP-depletion. Our data provide new insight into the molecular mechanism of preferential toxicity of Salinomycin towards cancer cells, and suggest possible clinical application of Salinomycin in combination with autophagy inhibitors (i.e. clinically-used Chloroquine). Furthermore, we discuss preferential Salinomycins toxicity in the context of Warburg effect.

1. Introduction

Salinomycin was originally used as an anticoccidial drug in poultry, and for efficient nutrient absorption in piggery. Its preferential toxicity towards cancer-stem cells was described by Gupta and colleagues in the end of the last decade [1]. Salinomycin's toxicity towards cancer stem cells was further supported by recent studies in gastrointestinal sarcoma, osteosarcoma, and colorectal and breast cancers [2–4]. Even though the cell death mechanisms induced by Salinomycin still remain elusive, a recent study by Lu et al. shows that Salinomycin targets cancer stem cells by blocking Wnt/β-catenin pathway, which is critical for stem cell self renewal [5]. While Salinomycin is relatively non-toxic to primary cells, Boehmerle et al., show that Salinomycin induced cell death is through conventional caspase mediated apoptotic pathways [6]. Our own experiments (please see below) show that Salinomycin preferentially kills cancer cells.

Cellular house-keeping, homeostatic mechanism autophagy includes macroautophagy (bulk degradation including cellular organelles), microautophagy (uptake of cytoplasm for degradation) and chaperone mediated autophagy (CMA) (protein specific degradation) [7–9]. In the

Abbreviations: ATG, Autophagy Related Gene; BCLN1, Beclin1; HMGB1, high mobility group binding protein 1; LC3, microtubule-associated protein 1 light chain 3; Mfn, mitofusin; MMP, mitochondrial membrane potential; mTOR, mammalian target of rapamycin; PGC1α, peroxisome proliferator-activated receptor gamma coactivator 1α; PTP, mitochondrial membrane permeability transition pore

* Corresponding author at: Dept. Clinical and Experimental Medicine (IKE), Integrative Regenerative Medicine Center (IGEN), Linköping University, Cell Biology Building, Level 10, 581 85 Linköping, Sweden. Tel.: +46 10 10 32787.
E-mail address: marek.los@liu.se (M.J. Łos).

0167-4889
http://dx.doi.org/10.1016/j.bbamcr.2013.04.011

presence of growth factors autophagy is inhibited by the activation of PI3K/Akt pathway through activation of mTOR (mammalian target of rapamycin) [10,11]. However, under nutrient deprivation or stress, inhibition of mTOR initiates phagophore formation through nucleation complex of autophagy involving ULK1/2, Beclin1 and other molecules. Several Autophagy Related Gene (ATG) family members ATG3, ATG5, ATG7, ATG12 etc., carry on further elongation of phagophore to form autophagosome [10,12]. Autophagosomes carry dysfunctional cellular organelles (mitochondria, peroxisomes, ribosomes etc.) for degradation by fusing with lysosomes. More recent studies show alternative autophagic pathway independent of ULK, ATG5 and ATG7 mediated mechanism-requiring Beclin1 [10,13,14]. Organelle specific autophagy has been reported for mitochondria (mitophagy), endoplasmic reticulum (ER-phagy), ribosomes (Ribophagy) etc., as a mechanism to remove the dysfunctional organelles, or as a response to stress triggered by cytoplasmic overload with damaged organelles[15].

Mitochondria, commonly called the powerhouses of the cell, form a dynamic interconnected network of tubular structures that are engaged in fission and fusion processes [16]. Mitochondrial fission is mediated by localization of Drp1 on the mitochondrial site of division whereas fusion is mediated by mitofusin proteins (mitofusins 1 and 2) along with OPA1 [17]. Lack of both mitofusin 1 (Mfn1) and mitofusin 2 (Mfn2) leads to impaired mitochondrial fusion but both of them can compensate each others loss [18–21]. Under the event of stress or any event leading to dysfunction of normal mitochondria, the organelle undergoes an asymmetric, protective fission, that aims to spare at least part of stressed mitochondria, by splitting the organelle into a normally-functioning part, and a dysfunctional one. The process allows for subsequent degradation of dysfunctional mitochondria created in such a way, while sparing the functional ones.

Rehman and colleagues have recently described that cancer cells often have much smaller, fragmented mitochondria as compared to normal cells [22]. In the same study they show that cancer cells express an increased level of Drp1 and decreased level of Mfn protein, promoting a constant mitochondrial fission with impaired fusion, resulting in a smaller fragmented mitochondria in cancer cells [22]. Modification of the level of expression of Drp1 or Mfn in cancer cells decreased their proliferation, thus indicating that targeting of molecules regulating mitochondrial dynamics and function is a potentially novel target for cancer therapy [22].

The maintenance of mitochondrial inner membrane potential is crucial for both ATP production and functions related to the induction of apoptosis. Opening of the outer mitochondrial membrane permeability transition pore (PTP) leads to cytochrome c release from the inter-membrane space of the mitochondria along with depolarization of the inner membrane and thus subsequently inhibiting the ATP production [23,24]. However it is argued that the mitochondrial membrane potential has to be maintained for the release of cytochrome c and further apoptotic signaling cascade to occur [25,26]. Others propose the mitochondrial hyperpolarization and thus mitochondrial condensation during apoptosis induction [27,28]. Irrespective of the mechanism, mitochondrial release of cytochrome c into the cytosol is the trigger and component for the formation of apoptosome that leads to the activation of caspase cascade. Along with apoptosis, autophagy may under certain circumstances act as an alternative cell death mechanism [29].

In this study, we have been investigating the mechanism of Salinomycin anticancer toxicity. Here we show that Salinomycin induces autophagy, and mitophagy. The autophagic response is a cell protective mechanism in prostate and breast cancer cells. We also report the critical role of Salinomycin in increasing the mitochondrial membrane potential (hyperpolarization) and activation of a programmed cell death through the differential activation of caspases among cancer cells. Our experimental data indicate that Salinomycin-triggered depletion of cellular ATP, in cancer cells but not in primary cells, contributes towards Salinomycin's preferential anticancer toxicity.

2. Materials and methods

2.1. Cells and cell culture

Prostrate cancer cell line (PC3), breast cancer cell lines (SKBR3 and MDAMB468) and murine embryonic fibroblast (MEF) cells, all available at our lab's cell bank, were cultured in RPMI media with 10% FBS and 1% penicillin–streptomycin antibiotics. MEF-ATG5$^{-/-}$ described previously [30], and human normal dermal fibroblasts, provided by Dr. Kratz [31], were cultured in DMEM media with 10% FBS and 1% penicillin. All the cell lines were maintained at a confluence of ~70%.

2.2. Materials and reagents

Salinomycin, Rapamycin, Bafilomycin, Chloroquine, Pepstatin and ED-64 were obtained from Sigma-Aldrich and dissolved in their respective buffers as per required concentrations. Rabbit-anti-LC3b, rabbit-anti-HMGB1, and murine anti-actin were also from Sigma-Aldrich whereas rabbit-anti-ATG5 was obtained from Cellular Signaling Inc. The secondary antibodies anti-rabbit HRP-conjugate and anti-murine HRP-conjugates were obtained from Sigma-Aldrich and anti-rabbit-Alexafluor488 and -594 were purchased from Life Technologies Ltd. MitoTracker Red CMXRos, LysoTracker Red DND-99, and MitoTracker Green FM were also purchased from Life Technologies Ltd.

2.3. Transmission electron microscopy (TEM)

Cells were initially fixed with 2% Glutaraldehyde in 0.1 M Sodium – cacodylate-HCl buffer with 0.1 M sucrose, (pH 7.4) for 2 h at 4 °C and post fixed with 1% OsO_4 in 0.15 M Sodium – cacodylate-HCl buffer for 1 h. Cells were dehydrated in ethanol gradually and embedded in Epon 812. Ultrathin sections were cut on a Reichert Ultracut S Ultramicrotome, mounted on copper grids, air-dried, and further stained with uranyl acetate and lead citrate. Sections were examined and photographed with JEOL JEM 1230 electron microscope at 100 kV [29].

2.4. MTT assay

100 μl of cells diluted at a concentration of 10^5 cells/ml were plated to each well of a 96 well plate and incubated in a humidified CO_2 chamber for 24 h. The next day, cells were treated as per respective experimental conditions (please see Results section and figure legends for details). After indicated time periods of treatments, 10 μl of 5 mg/ml 3-(4,5-dimethyl-2-thiazolyl) 2,5-diphenyl-2H tetrazolium bromide (MTT) solution (Sigma-Aldrich) was added to each well, incubated for 3 h and centrifuged at 90 *g* for 10 min. The supernatant was removed and the formed farmazan-crystals were dissolved in a solution containing equal volumes of DMSO:ethanol. The readings were taken at both 570 and 630 nm.

2.5. Po-Pro and 7-AAD cell death assay

Cells treated with or without Salinomycin at mentioned concentrations for the respective time periods were trypsinized and collected by centrifugation at 400 *g* for 5 min. The pelleted cells were resuspended in PBS and treated with Po-Pro and 7-AAD dyes (Life Technologies Ltd.) for 30 min as per manufacturer's instructions and analyzed using flow cytometer (Gallios, Beckman Coulter Inc.). Flow cytometry results were analyzed using Kaluza analysis software (Beckman Coulter Inc.).

2.6. Western blotting

Cells were lysed using RIPA buffer with Protease inhibitors (cOmplete Roche) and centrifuged to remove the debris. Cell lysates were loaded into a 12% polyacrylamide gel and ran at 100 V for 3 h and then

transferred on to a PVDF membrane for 1 h at 100 V. The membrane was blocked with 5% milk protein and treated with primary antibodies overnight. The membrane is washed with 3× TBST and treated with respective secondary antibody for 1 h. The membrane is further washed with 3× TBST before developing using Amersham ECL plus Western blotting developing kit (GE Technologies). To analyze HMGB1 release the cellular supernatant was collected and an equal amount of the supernatant was loaded into a 15% gel and Western blotting was conducted as described above [32].

2.7. Immunocytochemistry

Cells plated on cover-slips in a 12-well plate were washed with PBS after their respective treatment and fixed using 4% paraformaldehyde

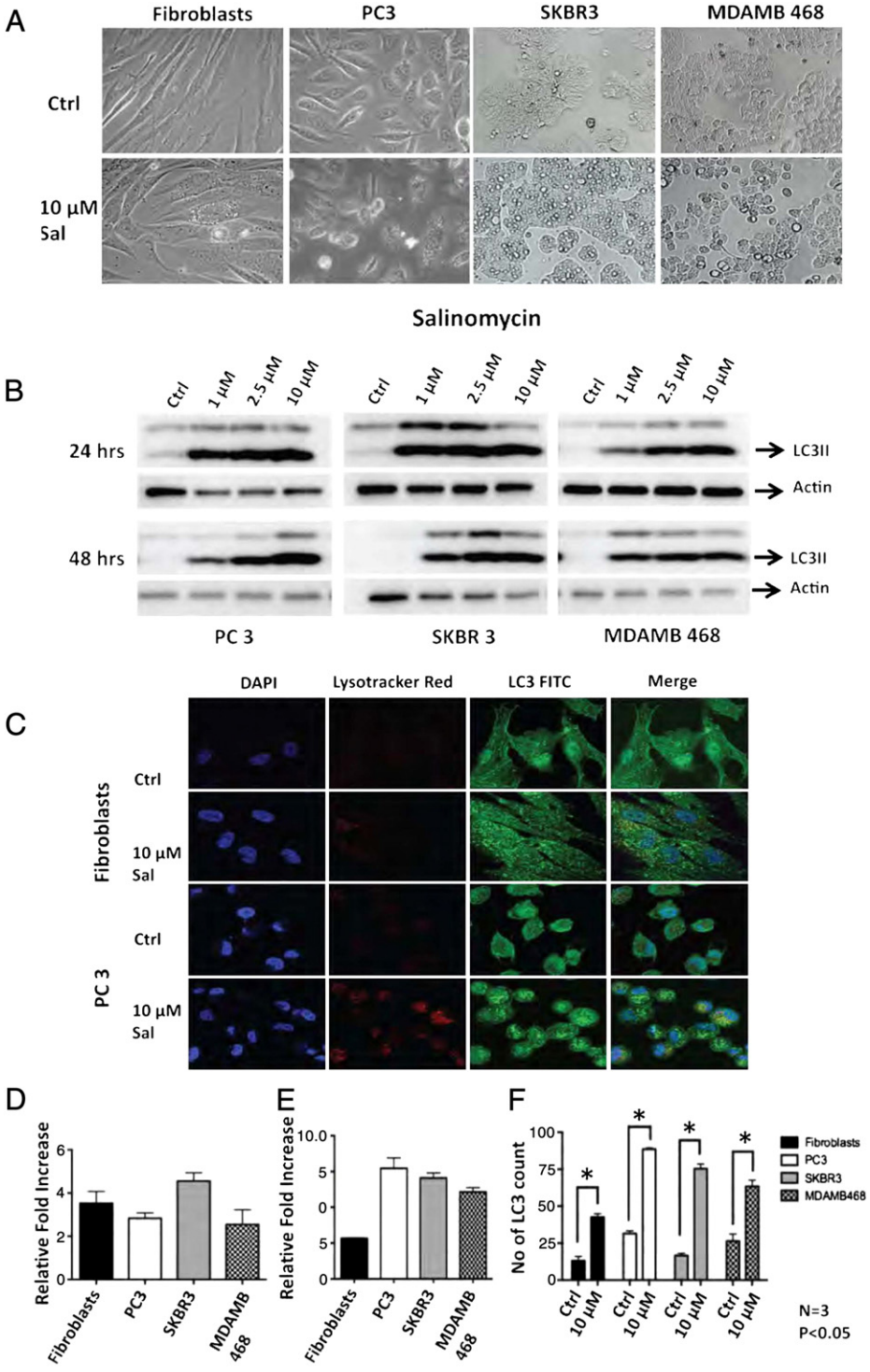

Fig. 1. Salinomycin treatment triggers autophagic response: (A) phase-contrast images show increased vacuolization in cancer cells treated with 10 μM Salinomycin (Sal). (B) Western blots show increased expression of LC3II upon treatment with mentioned concentrations of Salinomycin for 24 and 48 h in PC3, SKBR3 and MDAMB468 cells. (C) Colocalization of LC3 signal and LysoTracker representing autophagosome and lysosomes respectively was observed using immuno-cytochemistry in primary and cancer cells. (D, E, F) Quantitative evaluation of experiment depicted on "C": (D) 10 μM Salinomycin treatment increased number of cells showing higher than the threshold level of LC3 fluorescence compared to the respective controls, (E) number of LysoTracker Red counts per cell, and (F) number of LC3 signals per cell relative to their controls. *Represents statistically significant difference ($P < 0.05$).

for 20 min at 4 °C and rinsed twice with PBS for 5 min. The cells were then placed in incubation buffer (0.1% saponin and 5% FBS in PBS) for 20 min at room temperature and then treated with primary antibody (overnight at 4 °C) and respective secondary antibody with conjugated fluorophore (1 h at room temp.) intervened by 3× washing with incubation buffer. The cells were washed and then mounted on a slide with a mounting medium containing DAPI. Images were taken using Laser Scanning Confocal Microscope (Zeiss).

2.8. LC3 staining, LysoTracker count and mitochondrial count and size

Immunofluorescent images of the cells treated with and without Salinomycin and stained for LC3, LysoTracker, and MitoTracker probes as per the manufacturer's protocol were analyzed by ImageJ software subtracting the background, using threshold and analyzing particle modules as described in a previous study [22]. A total of 30 cells from each experiment are analyzed for LC3 positive cell count and a total of 10 cells were counted for the number of LC3 fluorescent dots and LysoTracker count. Mitochondrial size and count are analyzed using images taken at 3 random locations in each of the control and Salinomycin treated samples. To further determine the influence of autophagy on mitochondrial number the cells are selected based on LC3 positivity as mentioned above.

2.9. Mitochondrial membrane potential and mass measurement

Mitochondrial activity was measured with JC1 assay kit (Sigma-Aldrich). 200× JC1 stock solution was diluted with distilled water and 5× JC1 staining buffer as per the requirements to make 1× JC1 solution and is added to the cells either in suspension (for flow cytometry) or attached to the plate (fluorimetry) and incubated for 20 min at a 37 °C incubator. The cells were washed 2× with respective media and fluorescence was measured using a flow cytometer using FL1 and FL2 channels (Gallios, Beckman Coulter Inc.) or fluorescence plate reader (Victor3V, PerkinElmer) and images were taken using a confocal microscope (Zeiss). To further support the JC1 assay the same analysis using flow cytometry was performed with MitoTracker Green FM (localized to mitochondrial membrane and thus determine mitochondrial mass) and MitoTracker Red CMXRos that localizes to the matrix of the functional mitochondria with intact mitochondrial membrane potential (indicates mitochondrial function) as mentioned previously.

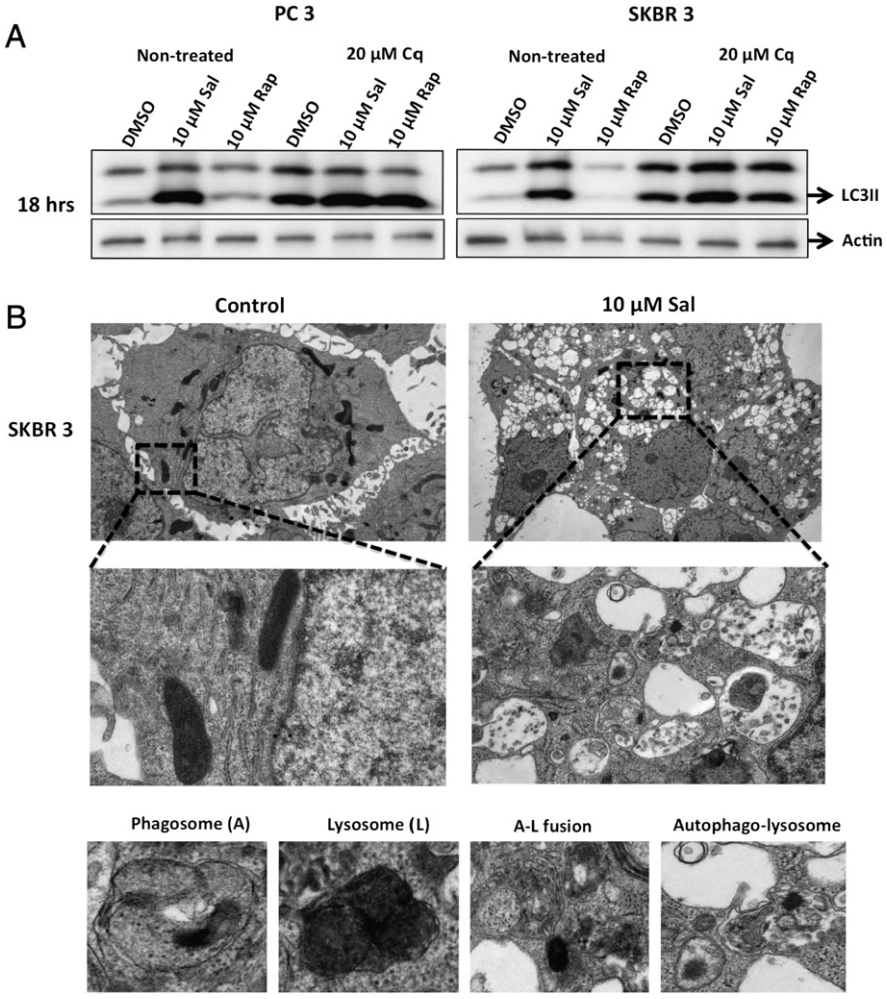

Fig. 2. Salinomycin increases LC3II flux upon inhibition of autophagy: (A) Western blotting was used to observe comparative expression of LC3II at different time intervals in the presence or absence of the autophagic inhibitor Chloroquine (Cq). Rapamycin (Rap), a well known autophagy inducer was used as a positive control for autophagy induction. Please note that Salinomycin induces a stronger autophagic response as compared to Rapamycin. Salinomycin treatment of cell pretreated with Cq shows upregulated LC3II expression compared to control non-treated cells. (B) TEM images of SKBR3 cells treated with or without Salinomycin for 24 h. Salinomycin treated cells show an increased number of autophagolysosome formed along with lysosomes and autophagosomes. Individual portraits of phagosomes and lysosomes were represented in the subpanel along with the images showing autophagosome and lysosome formation and matured autophagolysosome.

2.10. ATP assay

Cells treated with Salinomycin for the respective time periods were washed with ice-cold PBS and treated with 100 µl of ATP releasing agent (Sigma-Aldrich) for 5 min and 50 µl of the extract was added into a light protected 96-well plate that was preloaded with 100 µl of ATP assay mix solution (Sigma-Aldrich) and incubated for 3 min at room temp. Immediately the luminescence was measured using luminescence plate reader (Victor3V, PerkinElmer).

2.11. Caspase activity assays

Caspase-3 activity and mitochondrial function were assessed using NucView 488 and MitoView 633 (Biotium). Samples were prepared similarly as Po-Pro assay as described above and treated with NucView 488 and MitoView 633 and kept on ice for 1 h before analyzing with flow cytometer (Gallios). Caspase-8 and -9 were analyzed using Green FLICA and Red FLICA caspase assay kits respectively from ImmunoChemistry Technologies. The cells were incubated at 37 °C for 1 h before taking the fluorescence, which was measured in FL1 and FL4 using Gallios flow cytometer (Beckman Coulter Inc.).

2.12. Statistics

All the statistics (one way ANOVA) were conducted using Prism (version 6.0b) software and SPSS (IBM version 20) software. A P value of less than 0.05 is considered statistically significant unless mentioned otherwise.

3. Results

3.1. Salinomycin induces autophagy

Initial observations of 10 µM Salinomycin treated cells indicate a profound increase in vacuolization in breast cancer SKBR3 and MDAMB468 cell lines, and to lesser degree in prostate cancer PC3 cells, upon 24 h treatment (Fig. 1A). The vacuolization is much less pronounced in human normal dermal fibroblasts. To investigate possible autophagosome formation levels of autophagic marker LC3II were monitored in SKBR3, MDAMB468 and PC3 cells. As shown in Fig. 1B, Salinomycin treated cells have an increased level of LC3I lipidation and LC3II formation with different concentrations of Salinomycin (1 µM, 2.5 µM and 10 µM) at 24 and 48 h. Autophagy was also confirmed using immuno-cytochemistry (Fig. 1C, D and Supplementary Fig. 1) where 10 µM Salinomycin treated cells show an increase in the number of LC3 positive cells, number of LC3 fluorescent signals (fluorescent dots) per cell and the number of active lysosomes (using LysoTracker) per cell (Fig. 1D). Fig. 1C also shows a localization of active lysosomes (LysoTracker Red) and LC3 signal (green fluorescent dots) in the near vicinity (or colocalization) thus providing a strong evidence for an active autophagic mechanism. The relative number of lysosome increase (LysoTracker Red counts) per cell, is shown in Fig. 1E, whereas the relative number increase of LC3 signals per cell (increase in autophagosome formation relative to their controls), is shown in Fig. 1F.

To further support the increase in active autophagy in Salinomycin-treated cells, LC3II-flux was monitored at different time periods in prostate and breast cancer cell lines along with autophagy inhibitor. As predicted, an increase in LC3II accumulation was observed in Salinomycin treated cells that are pretreated for 1 h with autophagy inhibitor 20 µM Chloroquine (Fig. 2A, and Supplementary Fig. 2A). Similar observations were made using other autophagic inhibitors (Bafilomycin and pepstatin-ED64 mix) (Supplementary data Fig. 2B). Further validation of Salinomycin induced autophagic process was done by transmission electron microscopy (Fig. 2B and Supplementary Fig. 3). Salinomycin induces strong vacuolization and autophagosome formation. In the inset (bottom row) the representative images of lysosomes, autophagosomes and complete autophagolysosomes are indicated.

3.2. Salinomycin triggered autophagy counteracts cell death in cancer cells

Since autophagy may promote either cell survival or cell death, we tested by an MTT assay if autophagy inhibition by Chloroquine potentiates, or inhibits Salinomycin's toxicity. Surprisingly, inhibition of autophagy with Chloroquine (20 µM, Cq) in Salinomycin (10 µM, Sal) treated cancer cells increased cell death in tested breast- and prostate cancer cell lines, however, in human normal dermal fibroblasts autophagy inhibition actually increased survival (Fig. 3A). As shown in Fig. 3B, immortalized murine embryonic fibroblasts deficient in ATG5 (ATG5-KO), a crucial gene involved in autophagosome elongation, also show an increased cell death upon treatment with Salinomycin, as compared to the respective control wild-type fibroblasts (Fig. 3B).

3.3. Salinomycin treatment increases mitochondrial mass, and net mitochondrial membrane depolarization in cancer cells but not in primary cells, implications for cellular ATP-level

Our transmission electron microscopy data shown in Fig. 2B indicates that some Salinomycin triggered autophagosomes contained damaged

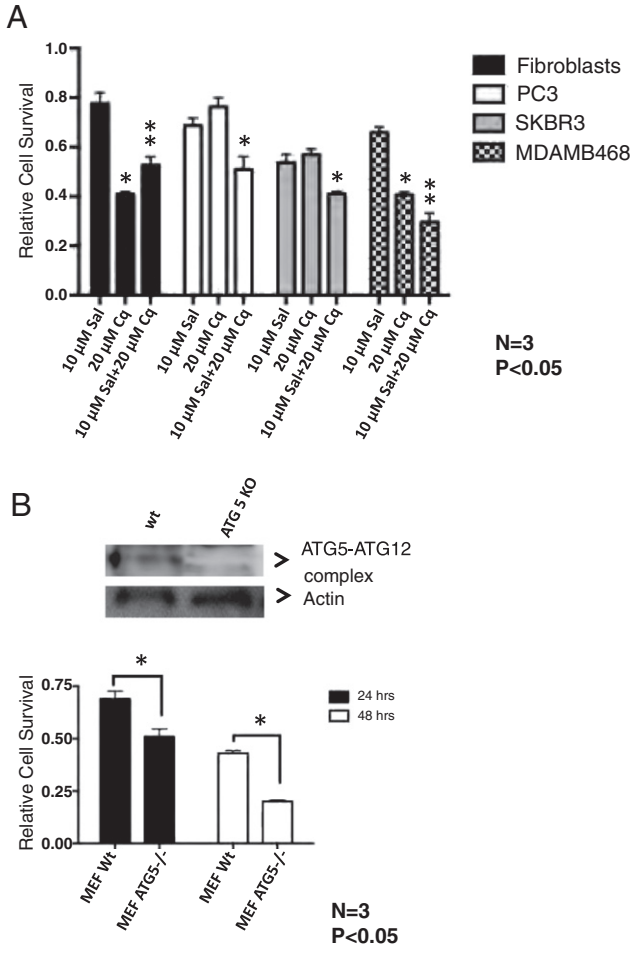

Fig. 3. Salinomycin induced autophagy promotes cancer cell survival: (A) inhibition of autophagy by Chloroquine increased cancer cell death triggered by Salinomycin. The effects on human normal dermal fibroblasts were inconclusive due to a marked toxicity of Chloroquine alone. (B) MEF cells lacking ATG5 showed significant increase in cell death compared to the respective controls at 24 h and 48 h. The Western blot shows ATG5 level in the respective cells lines (cell line quality controls). *Represents statistically significant difference ($P < 0.05$).

mitochondria. Thus, in order to assess the function of mitochondria and its role in Salinomycin induced cell death JC1 assay was used to analyze mitochondrial membrane potential and mitochondrial mass as described previously [33]. Using JC1 assay we can assess the net mitochondrial mass, represented by green signal, and intact mitochondrial potential represented by the red signal. As shown in Fig. 4AB, unlike human normal dermal fibroblasts, cancer cells treated with Salinomycin respond with the increase of mitochondrial mass (increased green fluorescence).

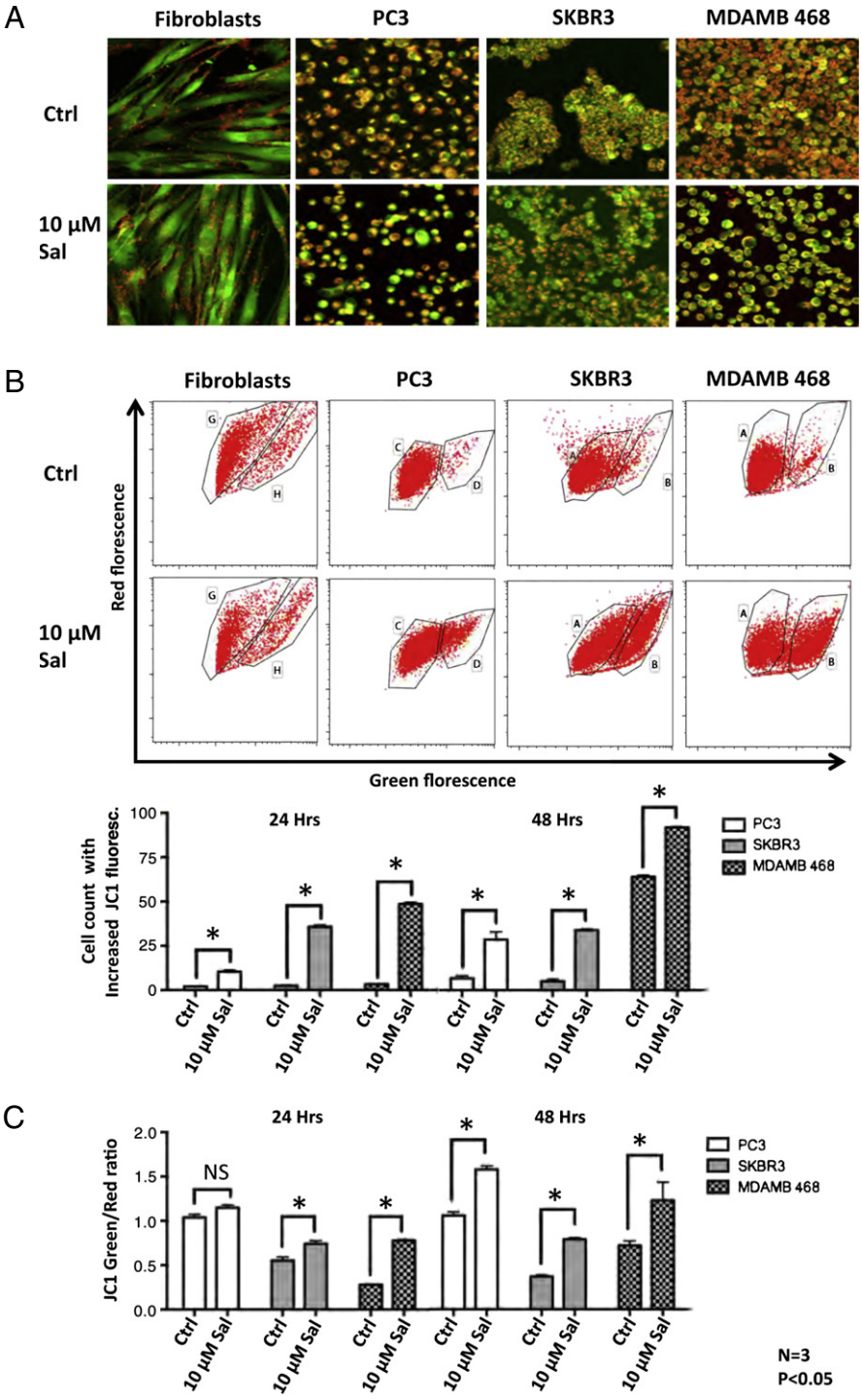

Fig. 4. Net mitochondrial depolarization observed among cells treated with Salinomycin is due to the increased mitochondrial mass; Salinomycin induces hyperpolarization in a subset of cells: (A) Confocal images show increase of green fluorescent signal upon Salinomycin treatment compared to controls, in cancer cell lines but in lesser extent among primary fibroblasts. (B) Change in JC1 green and red fluorescence in cells treated with Salinomycin for 24 h was detected by flow cytometer. Cancer cell lines (PC3, SKBR3 and MDAMB468) show a major increase in the number of cells with increased green fluorescence, while only a minor increase in red fluorescence could be detected. Logarithmic scales were used to display both parameters. Compensation was done using Kaluza software (Beckman Coulter Inc.). (C) Quantitative representation of JC1 (green to red) ratios obtained from flow cytometry. Cancer cells treated with Salinomycin show increased JC1 ratio compared to their respective controls. (D) Changes in the JC1 green fluorescence (indicates mitochondrial mass) and JC1 red fluorescence (indicating mitochondrial membrane potential) were monitored upon Salinomycin treatment for 24 h and 48 h. PC3, SKBR3 and MDAMB468 cells show an increase in both green and red fluorescence at 24 h and 48 h except MDAMB468 cells at 48 h that show a decrease in red fluorescence but increased green fluorescence. (E) Human normal dermal fibroblasts showing a decrease in JC1 ratio at 24 h but JC1 ratio is regained to normal by 48 h. (F) Salinomycin decreases the expression of MFN2 and increases the expression of DRP1, in SKBR3 cells. *Represents statistically significant difference ($P < 0.05$). NS = nonsignificant.

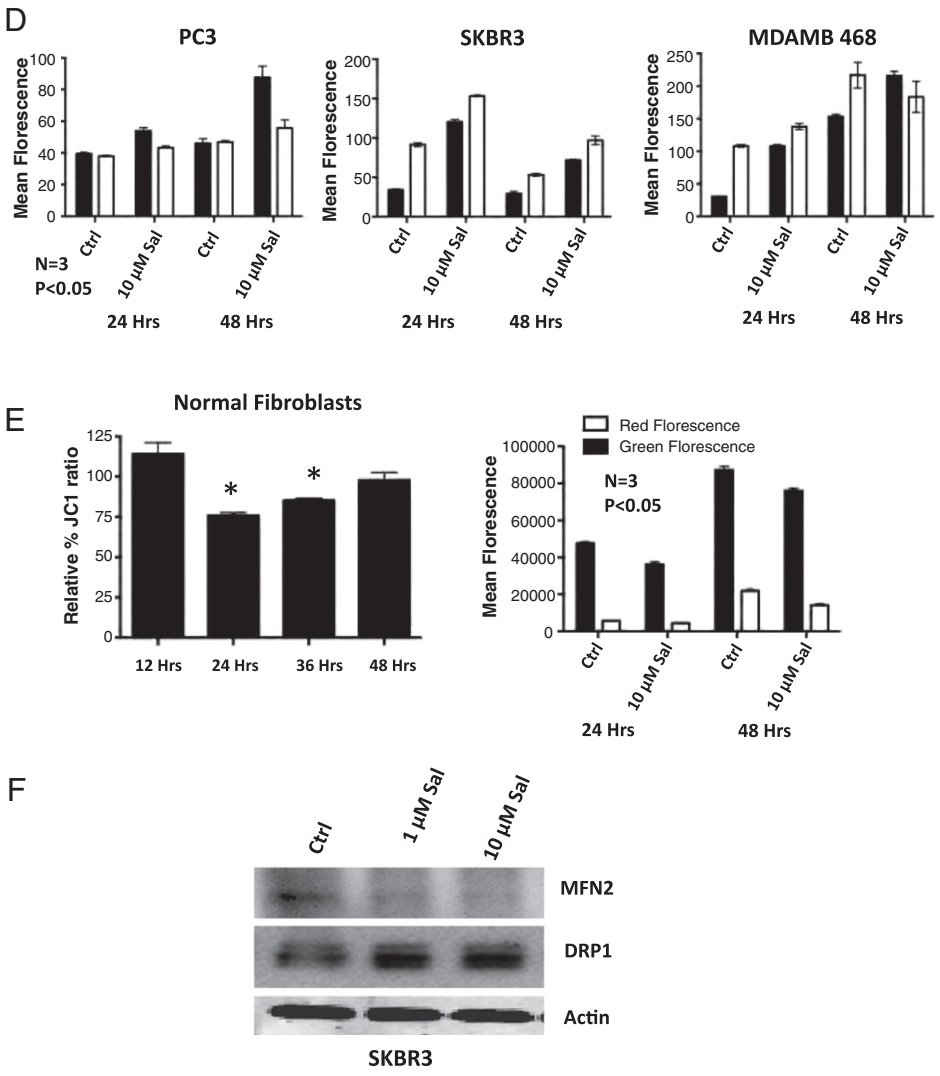

Fig. 4 (*continued*).

Fig. 4B bottom panel, represents quantification of flow cytometric data shown at the upper panel. JC1 signal quantification by flow cytometry (Fig. 4C, D) to analyze changes in mitochondrial function shows that there is an increase in both JC1 green and red fluorescence in breast cancer cell lines (SKBR3 and MDAMB468) at 24 h and 48 h with the exception that MDAMB468 cells show decreased red fluorescence at 48 h but increased green fluorescence (Fig. 4D). Prostate cancer PC3 cell lines show a strong increase in green fluorescence but no statistically significant changes in red fluorescence. Thus, Salinomycin treated cancer cells, when analyzed as a whole, show drastic increase in JC1 (green/red) ratio (Fig. 4C) indicating a net increase in depolarized mitochondria. However, Fig. 4B clearly shows the appearance of subpopulation of cancer cells with a strong red signal (hyperpolarized mitochondria), upon Salinomycin treatment. In fibroblasts, JC1 red fluorescence does not change significantly under Salinomycin treatment at 24 h and 48 h, however green fluorescence shows a very significant decrease at 24 h and a partial decrease at 48 h thus causing a decrease in JC1 ratio initially with the signs of JC1 ratio recovery to normalcy by 48 h (Fig. 4E). The observed changes in mitochondria by confocal fluorescence microscopy correspond in decreased expression of MFN2 and increased expression of DRP1 upon Salinomycin treatment, as shown by Western blot (Fig. 4F).

Similar results were obtained using MitoTracker Green FM and MitoTracker Red CMXRos dyes that indicate similar parameters as that of JC1 green and JC1 red fluorescence respectively. As shown in Supplementary Fig. 4, MitoTracker Red and MitoTracker Green signals increased in Salinomycin treated cells compared to the control cells. Consistent to the JC1 ratio data MitoTracker Green fluorescence increased more drastically compared to MitoTracker Red, thus further supporting a marked increase in mitochondrial mass combined with a significant, net decrease in mitochondrial polarity.

To gain further insight into the functional state of mitochondria, we measured ATP-levels in primary cells and cancer cells treated with Salinomycin. A steady decrease in the amount of ATP levels was observed in both prostate cancer PC3 cell line and breast cancer SKBR3 and MDAMB468 cells (Fig. 5) treated with 10 μM Salinomycin for 12, 24, 36 and 48 h. However, there was no such alteration observed in human normal dermal fibroblasts (Fig. 5).

3.4. Salinomycin disrupts mitochondrial network and induces mitophagy

Salinomycin treated cells showed various mitochondrial abnormalities and mitoptotic changes (Fig. 6A, and Supplementary Fig. 6A) [34]. Furthermore, EM-micrographs indicate that mitochondria (in addition to previously reported ER role in this capacity) may be the sources of membranes for the formation of autophagosomes, as a conspicuous number of mitochondria like structures showed encapsulated darkly stained lysosomal-like bodies (Supplementary Fig. 6B) [35]. Electron micrographs also showed relatively shorter mitochondria in the Salinomycin treated cells (Fig. 6A), as compared to the

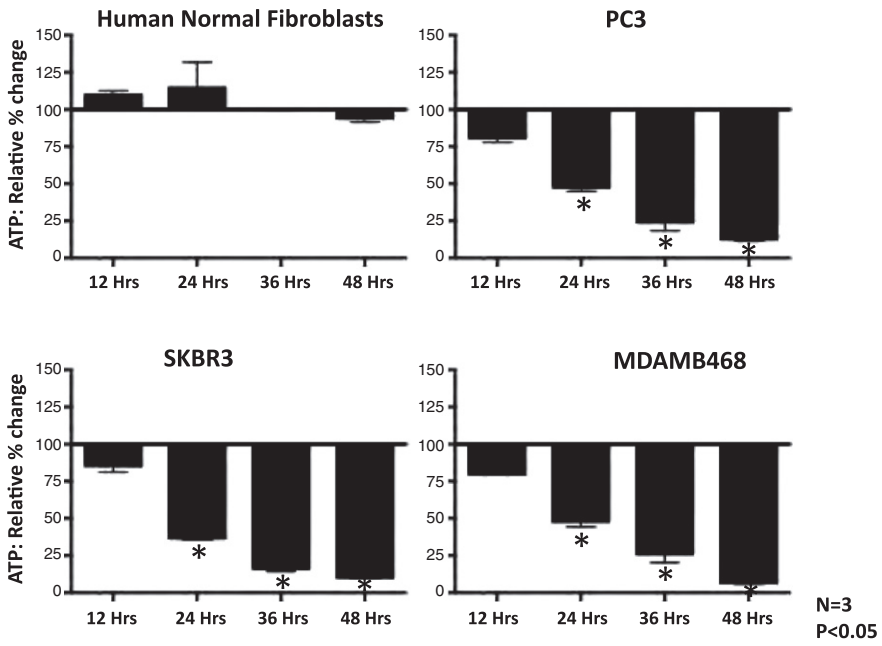

Fig. 5. Salinomycin treatment of cancer cells triggers decrease in ATP content: total ATP levels were measured in human normal dermal fibroblasts and cancer cells, upon treatment with 10 μM Salinomycin. ATP-level was not changed in human normal dermal fibroblasts upon Salinomycin treatment, however the same Salinomycin treatment causes a strong, time-dependent ATP-depletion in cancer cell lines. *Represents statistically significant difference ($P < 0.05$).

more elongated mitochondria in respective control non-treated cells. A manual count of total mitochondria per cell using electron micrographs also showed a decrease in the number of mitochondria with intact morphological features (Fig. 5B). In accordance with the electron microscopy data, a careful analysis of confocal images obtained for treated and non-treated cancer cells stained with MitoTracker Red CMXRos indicates mitochondria with intact mitochondrial potential. Furthermore, we observe a lower number of mitochondria with increased size (Fig. 5C, D, and Supplementary Fig. 7) that may be indicative for mitochondrial swelling.

Mitochondrial autophagy was further confirmed by LC3 signal colocalization with the mitochondria (MitoTracker Red) in both primary and cancer cells treated with 10 μM Salinomycin (Fig. 6E). In the same figure, Salinomycin treated cells show disruption in the mitochondrial network and relatively shorter mitochondria in fibroblasts and swollen or clumped mitochondria in cancer cell lines (Fig. 6E, and Supplementary Fig. 8).

3.5. Salinomycin-induced cell death form, depends on drug's concentration

As indicated by MTT assay results (Fig. 7A), Salinomycin induced a higher level of cell death in cancer cells as compared to human normal dermal fibroblasts (control). Since MTT assay does not distinguish between forms of cell death (it is a cell survival assay) we have next probed cell death induced by Salinomycin, using flow-cytometric 7AAD/Po-Pro assay that allows distinguishing between necrosis and apoptosis. As shown in Fig. 7B, cancer cells treated with lower concentration of Salinomycin (1 μM) show an increased number of early apoptotic cells (increase in only Po-Pro staining) and dead cells/necrotic cells (positive for Po-Pro and 7AAD stains). However, at higher concentration of Salinomycin (10 μM), along with apoptotic population, a significant number of cells show increased 7AAD staining without Po-Pro staining indicating a direct induction of necrotic cell death (Fig. 7B). Salinomycin-induced necrosis was further confirmed by detecting HMGB1 in cell medium (HMGB1 normally resides in cell nucleus, if found in cell medium, it is considered a necrotic marker). Treatment of cancer cells with Salinomycin, increased medium content of HMGB1 in a dose-dependent manner (Fig. 7C). Unlike in cancer cells, no marked increase in cell death was observed in human normal dermal fibroblasts treated with 10 μM Salinomycin (Fig. 7D).

3.6. Salinomycin triggers caspase mediated apoptosis among the cells showing hyperpolarized mitochondria

We have previously shown (Fig. 4B) that a subset of cancer cells treated with Salinomycin responds with mitochondrial hyperpolarization, rather than depolarization. Thus, we next checked the effects of Salinomycin on caspase-3 activity in our cell line models, while costaining them with MitoView 633 (indicator for polarized mitochondria). Flow-cytometric data indicate a significant increase in number of cells with increased mitochondrial polarization upon treatment with 1 μM Salinomycin for 24 h in SKBR3 and MDAMB468 cells (Fig. 8AB). Surprisingly, we have observed a significant increase in caspase-3 activity predominantly in cells showing hyperpolarized mitochondria (MitoView 633-high) in Salinomycin treated cells compared to their controls (Fig. 8B). Similarly, Salinomycin treated cells showed an increase in caspase-9 and caspase-8 activities compared to the controls (Fig. 8B). Furthermore inhibition of caspase activity using a pan-caspase inhibitor quinoline-Val-Asp(Ome)-CH2-O-phenoxy (Q-VD-OPh, 10 μM) showed partial rescue from cell death by Salinomycin among SKBR3 cells (Fig. 8C).

4. Discussion

Improving understanding of the biology of cancer, as well as new experimental drugs, like Salinomycin, that preferentially target cancer stem cells brings us closer to finding cure against this devastating group of diseases. Cancer biology is complicated and each type of cancer harbors its individual changes that may further evolve, once clinical therapy progresses. Still, some core aspects of cancer biology are prevalent in different forms of cancer. Among them are: (*i*) the presence of cancer stem cells (CSC) (tumor initiating cells) in (almost) every cancer, and (*ii*), set of metabolic changes, and anomalies in mitochondrial biology (Warburg effect), that make cancer metabolism largely dependent

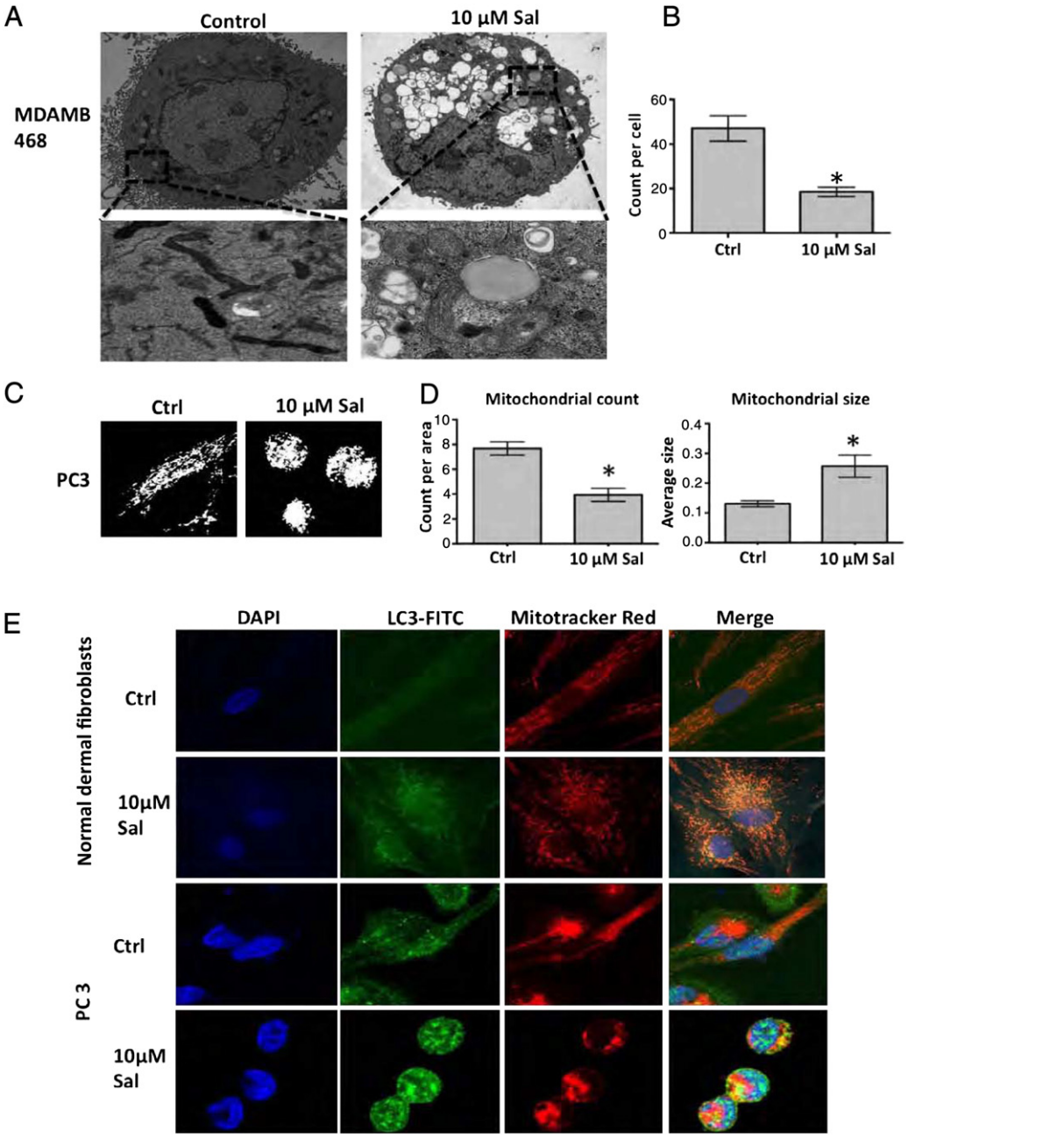

Fig. 6. Salinomycin induces alteration in mitochondrial tubular network and triggers mitophagy: (A) TEM pictures showing Salinomycin induced mitochondrial fragmentation. (B) Salinomycin decreases the number of functional mitochondria in treated cancer cells. (C) Representative images of ImageJ analysis by setting a threshold and quantifying the MitoTracker Red stained cancer cells, (D) which also shows a decrease in mitochondrial count but with increase in mitochondrial size (possible swelling). (E) Mitochondrial autophagy: colocalization of LC3 signal with mitochondria (MitoTracker Red) shown in the confocal images. *Represents statistically significant difference ($P < 0.05$).

on glycolysis [36]. In this project, we focused on better understanding of the mechanism of Salinomycin toxicity, which as mentioned earlier [1], preferentially kills cancer stem cells. We observed that Salinomycin triggered an increase in autophagy (as shown with the increased LC3 flux, number of lysosomes and formation of autophagolysosomes) in both, cancer cell lines (prostate and breast cancer cells) and primary cells (human normal dermal fibroblasts). The autophagy induced by Salinomycin was much stronger than by Rapamycin, which is typically used as a "positive control" for autophagy experiments. Salinomycin induced autophagy acts as a cell protective mechanism in cancer cells as ablation of autophagy with either autophagic inhibitors (Chloroquine) or experiments involving Salinomycin treatment of murine fibroblasts deficient in ATG5 ($ATG5^{-/-}$) showed increased cell death. Interestingly, the increase of Salinomycin's toxicity upon autophagy inhibition was observed in breast and prostate cancer cells, but not in human normal dermal fibroblasts. This observation once again supports the popular understanding that autophagy is primarily a cell survival pathway, but if excessive, it may kill the cells [37].

The molecular mechanism of Salinomycin's toxicity is complex and involves several effects. The increasing evidence of restoration to normal mitochondrial function and subsequent mitigation to promote oxidative phosphorylation as a means to meet cellular energy needs among cancer cells is considered an adequate move to overhaul their apoptotic resistance. In line to the role of mitochondria at the center of Salinomycin induced cell death we have observed several abnormal mitochondrial phenotypes and mitochondrial specific localization of autophagy marker

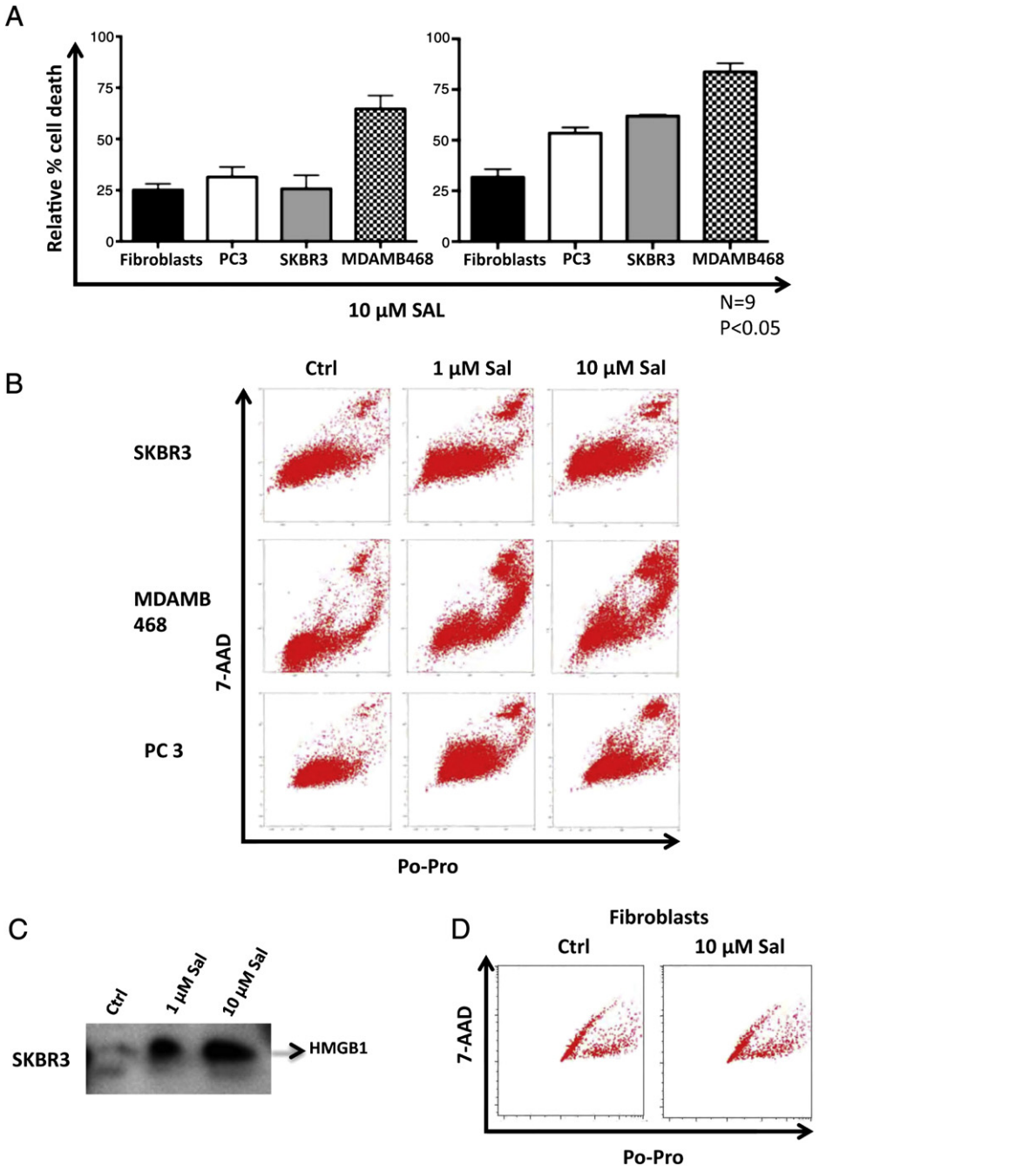

Fig. 7. Salinomycin induces both apoptosis and necrotic-like cell death: (A) MTT assay shows an increase in cell death in cells treated Salinomycin for 24 h and 48 h (please note relative resistance of human normal dermal fibroblasts to Salinomycin). (B) At low concentrations (1 µM) Salinomycin induces apoptosis (cells showing increase in Po-Pro staining) and dead cells. (B) At a high concentration, Salinomycin triggers 2 different forms of cell death: for Po-Pro positive (apoptotic), and necrotic with increased staining for 7-AAD only; a third population of cells (positive for both Po-Pro and 7-AAD) represent dead cells that are either late necrotic, or may have entered secondary necrosis. (C) Western blotting of supernatants of the SKBR3 cells treated with 1 µM and 10 µM Salinomycin shows increased release of necrotic marker HMGB1 among cells treated with 10 µM Salinomycin compared to both control and 1 µM Salinomycin treated cells. (D) Human normal dermal fibroblasts treated with 10 µM Salinomycin for 48 h show no marked increase in staining for apoptotic or necrotic markers. Logarithmic scales were used to display both parameters. Compensation was not applied (no emission spectra overlap).

LC3 indicating mitophagy. Mitochondrial tubular network showed disintegration along with fragmentation, the result of mitochondrial dynamics of fission and fusion, upon Salinomycin treatment. Both fission and fusion assist cellular stress rescue with mitochondrial fusion restoring the minimally damaged mitochondria and fission resulting in the cleavage of mitochondria followed by degradation of the damaged mitochondrial portion [16]. Similarly, Salinomycin treatment to cancer cells showed decreased number of mitochondria with intact inner membrane potential, increased staining for MitoTracker Red, a marker for intact inner mitochondrial membrane potential ($\Delta\Psi$) along with increased mitochondrial mass (marked by increased JC1 green fluorescence and MitoTracker Green FM). Moreover, there is no change in PGC1α protein expression, a major regulator for nuclear initiated mitochondrial biogenesis, upon treatment with Salinomycin in cancer cell lines (Supplementary Fig. 9); thus, inferring that mitochondrial dynamic fusion and fission mechanisms contribute to the alterations in mitochondrial mass and maintenance of mitochondrial function in Salinomycin treated cells. While we interpret the increase of JC1 green fluorescence

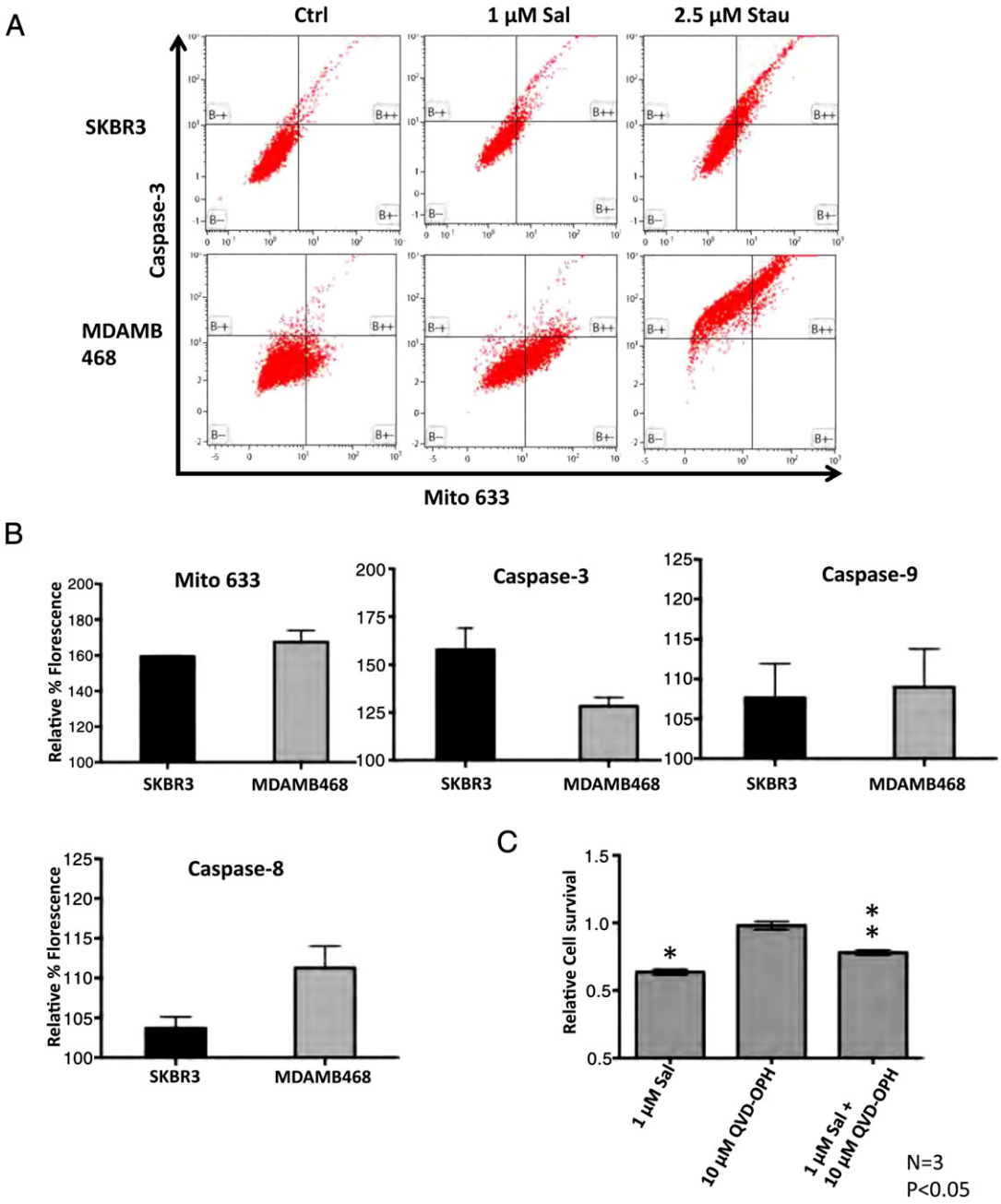

Fig. 8. Salinomycin triggers caspase activity among cells with hyperpolarized mitochondria: (A) Flow cytometric analysis for caspase-3 activity and mitochondrial polarization (MitoView 633) shows an increase in caspase-3 along with hyperpolarization in cancer cells treated with 1 μM Salinomycin for 24 h. Staurosporine (positive control) treatment of cancer cells also showed similar hyperpolarization of mitochondria along with caspase-3 activity. (B) Quantification of flow cytometric data shows increase in activities of caspase-3, -8, and -9 along with mitochondrial polarization in Salinomycin treated cells. (C) Inhibition of caspase activity using pan-caspase inhibitor Q-VD-OPh (10 μM) partially counteracted Salinomycin induced cell death. *Represents statistically significant difference ($P < 0.05$).

and MitoTracker Green staining as mitochondrial mass increase, one cannot fully exclude the possibility that the signal increase by both staining procedures is due to mitochondrial swelling.

Salinomycin treated cancer cells showed a decreased number of mitochondria with intact $\Delta\Psi$ and increased staining for mitochondrial polarity in a subpopulation of cancer cells. We have also observed an increase in mitochondrial mass along with co-localization of LC3 with the mitochondria and TEM images showing various abnormal mitochondrial phenotypes. The dysfunctional mitochondria are either eliminated by mitophagy or contributed the membrane to autophagosomes to further encapsulate lysosomes and form autophago-lysosomes. This is an important pro-survival mechanism, since dysfunctional mitochondria may actually consume ATP, and/or generate excessive amounts of harmful reactive oxygen species, thus contributing to loss of cellular homeostasis [38].

Similar to the hyperpolarization of mitochondria by Salinomycin in cancer cells, early studies using mitochondria isolated from rat liver Mitani et al., showed that Salinomycin increases release of K^+ ions from the mitochondria opposing the valinomycin induced depolarization of mitochondria by the uptake of K^+ ions [39]. In the same study Mitani et al., show that Salinomycin mediated inhibition of oxidative phosphorylation is K^+ ion dependent [39]. Likewise, in our current study cancer cells treated with Salinomycin showed depletion in total cellular ATP in a time and concentration dependent manner. ATP-depletion itself may be a strong autophagy-inducing stimulus, as the cell tries to restore its ATP-level [40,41].

Mitochondrial hyperpolarization was also reported in staurosporine-, Fas- and p53-triggered apoptosis [25,27,28,42,43]. However, human normal dermal fibroblasts did not show such depletion in ATP upon treatment with Salinomycin. The observed cancer cell specific deleterious effect of Salinomycin is explained by the fact that cancer cells harbor various abnormalities within mitochondria, such as hyperpolarized mitochondria along with defective mitochondrial fission and fusion mechanisms due to the lack of functionally intact mitofusin proteins, DRP1 and other proteins involved in the mitochondrial dynamics [22,44]. This compromised mitochondrial function among cancer cells could be the major contributor for the susceptibility of cancer cells to the ionic fluctuations induced by Salinomycin. Moreover, Dichloroacetate (DCA), which is also a K^+ ion channel modulator, and a molecule that preferentially targets cancer cells, contrasting to Salinomycin induces depolarization of mitochondria [44,45]. Thus, ionic manipulation within mitochondria offers a unique target for the development of novel cancer therapies.

Similar to staurosporine, Salinomycin also triggered activation of executioner caspase-3 along with initiator caspase-9, but only among the cells with hyperpolarized mitochondria. Inhibition of caspases using pan-caspase inhibitor Q-VD-OPh partially protected from cell death induced by Salinomycin but it was unable to fully reverse Salinomycin's toxic effect. Besides the activation of apoptotic signaling pathways, we also observed necrotic/necroptotic cell death, especially among cancer cells treated with higher concentrations (10 μM) of Salinomycin. A subpopulation of cells showed increased staining with 7-AAD, which in the used method preferentially stains necrotic cells, without any staining with an apoptotic marker (Po-Pro). Necrosis/necroptosis induction was also confirmed by the detection of HMGB1 protein (necrotic marker) [46,47] in the extracellular supernatant of cells treated with higher concentrations of Salinomycin.

Numerous manuscripts published within the recent decade, clearly show that a number of cell death stimuli simultaneously activate apoptosis, necrosis (or necroptosis) and autophagy [8]. Apoptosis however, as the most specialized form of cell death usually prevails, not only due to its speed, but also because caspases actively cleave and eliminate elements of necrotic or autophagic machinery [15]. For example, caspases cleave and inactivate key elements of autophagic machinery, Beclin1, ATG4 and ATG5 [10,29,48]. Generated in the process fragments, i.e. the C-terminal Beclin1 fragment gains the ability to amplify mitochondrion-dependent apoptosis despite a lack of a BH3 domain [49]. Furthermore, Bcl2 anti-apoptotic proteins (Bcl2/Bcl-XL) can attach to Beclin1 and inhibit autophagy. Concomitantly, caspase-8 may block necrosis or necroptosis by the cleavage of RIPK1 and RIPK3, and thus, prevent the formation of a necrosome [50].

In conclusion, this study shows that: (*i*) Salinomycin induces autophagy that initially has a protective effect in cancer cells, (*ii*) Salinomycin triggers mitochondrial swelling, mitophagy and disrupts mitochondrial architecture, (*iii*) cancer cell specific toxicity of Salinomycin is through mitochondrial hyperpolarization observed preferentially in cancer cells, (*iv*) Salinomycin induces both, caspase mediated apoptosis and necrosis/necroptosis as evident by the release of HMGB1, and (*v*) Salinomycin caused strong and time-dependent ATP-depletion in cancer cells, but not in human normal dermal fibroblasts. Thus, specific and more robust toxicity of Salinomycin towards cancer and cancer stem cells without much adversity towards normal cells warrants the use of Salinomycin as an effective chemotherapeutic agent, in combination with autophagy inhibitors.

Acknowledgements

SG was supported by Parker B Francis fellowship in Respiratory Disease. MJL and JRJ kindly acknowledge the core/startup support from Linköping University, from Integrative Regenerative Medicine Center (IGEN), from Cancerfonden (CAN 2011/521), and from VR-NanoVision (K2012-99X-22325-01-5).

Appendix A. Supplementary data

Supplementary data to this article can be found online at http://dx.doi.org/10.1016/j.bbamcr.2013.04.011.

References

[1] P.B. Gupta, T.T. Onder, G. Jiang, K. Tao, C. Kuperwasser, R.A. Weinberg, E.S. Lander, Identification of selective inhibitors of cancer stem cells by high-throughput screening, Cell 138 (2009) 645–659.
[2] P.S. Oak, F. Kopp, C. Thakur, J.W. Ellwart, U.R. Rapp, A. Ullrich, E. Wagner, P. Knyazev, A. Roidl, Combinatorial treatment of mammospheres with trastuzumab and salinomycin efficiently targets HER2-positive cancer cells and cancer stem cells, Int. J. Cancer 131 (2012) 2808–2819.
[3] Y. Wang, Effects of salinomycin on cancer stem cell in human lung adenocarcinoma A549 cells, Med. Chem. 7 (2011) 106–111.
[4] Q.M. Zhi, X.H. Chen, J. Ji, J.N. Zhang, J.F. Li, Q. Cai, B.Y. Liu, Q.L. Gu, Z.G. Zhu, Y.Y. Yu, Salinomycin can effectively kill ALDH(high) stem-like cells on gastric cancer, Biomed. Pharmacother. 65 (2011) 509–515.
[5] D. Lu, M.Y. Choi, J. Yu, J.E. Castro, T.J. Kipps, D.A. Carson, Salinomycin inhibits Wnt signaling and selectively induces apoptosis in chronic lymphocytic leukemia cells, Proc. Natl. Acad. Sci. U. S. A. 108 (2011) 13253–13257.
[6] A. Huczynski, Salinomycin: a new cancer drug candidate, Chem. Biol. Drug Des. 79 (2012) 235–238.
[7] S.M. Alavian, S.R. Ande, K.M. Coombs, B. Yeganeh, P. Davoodpour, M. Hashemi, M. Los, S. Ghavami, Virus-triggered autophagy in viral hepatitis — possible novel strategies for drug development, J. Viral Hepat. 18 (2011) 821–830.
[8] W. Chaabane, S.D. User, M. El-Gazzah, R. Jaksik, E. Sajjadi, J. Rzeszowska-Wolny, M.J. Los, Autophagy, apoptosis, mitoptosis and necrosis: interdependence between those pathways and effects on cancer, Arch. Immunol. Ther. Exp. 61 (2013) 43–58.
[9] B. Yeganeh, S. Mukherjee, L.M. Moir, K. Kumawat, H.H. Kashani, R.A. Bagchi, H.A. Baarsma, R. Gosens, S. Ghavami, Novel non-canonical TGF-beta signaling networks: emerging roles in airway smooth muscle phenotype and function, Pulm. Pharmacol. Ther. 26 (2012) 50–63.
[10] B. Levine, Cell biology: autophagy and cancer, Nature 446 (2007) 745–747.
[11] S. Ghavami, B. Yeganeh, G.L. Stelmack, H.H. Kashani, P. Sharma, R. Cunnington, S. Rattan, K. Bathe, T. Klonisch, I.M. Dixon, D.H. Freed, A.J. Halayko, Apoptosis, autophagy and ER stress in mevalonate cascade inhibition-induced cell death of human atrial fibroblasts, Cell Death Dis. 3 (2012) e330.
[12] S. Ghavami, R.H. Cunnington, B. Yeganeh, J.J. Davies, S.G. Rattan, K. Bathe, M. Kavosh, M.J. Los, D.H. Freed, T. Klonisch, G.N. Pierce, A.J. Halayko, I.M. Dixon, Autophagy regulates trans fatty acid-mediated apoptosis in primary cardiac myofibroblasts, Biochim. Biophys. Acta 1823 (2012) 2274–2286.
[13] Y. Nishida, S. Arakawa, K. Fujitani, H. Yamaguchi, T. Mizuta, T. Kanaseki, M. Komatsu, K. Otsu, Y. Tsujimoto, S. Shimizu, Discovery of Atg5/Atg7-independent alternative macroautophagy, Nature 461 (2009) 654–658.
[14] H. Cheong, T. Lindsten, J. Wu, C. Lu, C.B. Thompson, Ammonia-induced autophagy is independent of ULK1/ULK2 kinases, Proc. Natl. Acad. Sci. U. S. A. 108 (2011) 11121–11126.
[15] M.V. Jain, A.M. Paczulla, T. Klonisch, F.N. Dimgba, S.B. Rao, K. Roberg, F. Schweizer, C. Lengerke, P. Davoodpour, V.R. Palicharla, S. Maddika, M. Los, Interconnections between apoptotic, autophagic and necrotic pathways: implications for cancer therapy development, J. Cell. Mol. Med. 17 (2013) 12–29.
[16] R.J. Youle, A.M. van der Bliek, Mitochondrial fission, fusion, and stress, Science 337 (2012) 1062–1065.
[17] G. Benard, M. Karbowski, Mitochondrial fusion and division: regulation and role in cell viability, Semin. Cell Dev. Biol. 20 (2009) 365–374.
[18] T. Koshiba, S.A. Detmer, J.T. Kaiser, H. Chen, J.M. McCaffery, D.C. Chan, Structural basis of mitochondrial tethering by mitofusin complexes, Science 305 (2004) 858–862.
[19] S. Frank, B. Gaume, E.S. Bergmann-Leitner, W.W. Leitner, E.G. Robert, F. Catez, C.L. Smith, R.J. Youle, The role of dynamin-related protein 1, a mediator of mitochondrial fission, in apoptosis, Dev. Cell 1 (2001) 515–525.
[20] N. Taguchi, N. Ishihara, A. Jofuku, T. Oka, K. Mihara, Mitotic phosphorylation of dynamin-related GTPase Drp1 participates in mitochondrial fission, J. Biol. Chem. 282 (2007) 11521–11529.
[21] H. Chen, S.A. Detmer, A.J. Ewald, E.E. Griffin, S.E. Fraser, D.C. Chan, Mitofusins Mfn1 and Mfn2 coordinately regulate mitochondrial fusion and are essential for embryonic development, J. Cell Biol. 160 (2003) 189–200.
[22] J. Rehman, H.J. Zhang, P.T. Toth, Y. Zhang, G. Marsboom, Z. Hong, R. Salgia, A.N. Husain, C. Wietholt, S.L. Archer, Inhibition of mitochondrial fission prevents cell cycle progression in lung cancer, FASEB J. 26 (2012) 2175–2186.
[23] M. Los, S. Wesselborg, K. Schulze-Osthoff, The role of caspases in development, immunity, and apoptotic signal transduction: lessons from knockout mice, Immunity 10 (1999) 629–639.
[24] D.D. Newmeyer, S. Ferguson-Miller, Mitochondria: releasing power for life and unleashing the machineries of death, Cell 112 (2003) 481–490.
[25] J.L. Scarlett, P.W. Sheard, G. Hughes, E.C. Ledgerwood, H.H. Ku, M.P. Murphy, Changes in mitochondrial membrane potential during staurosporine-induced apoptosis in Jurkat cells, FEBS Lett. 475 (2000) 267–272.
[26] N.J. Waterhouse, J.C. Goldstein, O. von Ahsen, M. Schuler, D.D. Newmeyer, D.R. Green, Cytochrome c maintains mitochondrial transmembrane potential and ATP generation after outer mitochondrial membrane permeabilization during the apoptotic process, J. Cell Biol. 153 (2001) 319–328.

[27] M. Poppe, C. Reimertz, H. Dussmann, A.J. Krohn, C.M. Luetjens, D. Bockelmann, A.L. Nieminen, D. Kogel, J.H. Prehn, Dissipation of potassium and proton gradients inhibits mitochondrial hyperpolarization and cytochrome c release during neural apoptosis, J. Neurosci. 21 (2001) 4551–4563.
[28] R.M. Kluck, M.D. Esposti, G. Perkins, C. Renken, T. Kuwana, E. Bossy-Wetzel, M. Goldberg, T. Allen, M.J. Barber, D.R. Green, D.D. Newmeyer, The pro-apoptotic proteins, Bid and Bax, cause a limited permeabilization of the mitochondrial outer membrane that is enhanced by cytosol, J. Cell Biol. 147 (1999) 809–822.
[29] S. Ghavami, M.M. Mutawe, P. Sharma, B. Yeganeh, K.D. McNeill, T. Klonisch, H. Unruh, H.H. Kashani, D. Schaafsma, M. Los, A.J. Halayko, Mevalonate cascade regulation of airway mesenchymal cell autophagy and apoptosis: a dual role for p53, PLoS One 6 (2011) e16523.
[30] A. Kuma, M. Hatano, M. Matsui, A. Yamamoto, H. Nakaya, T. Yoshimori, Y. Ohsumi, T. Tokuhisa, N. Mizushima, The role of autophagy during the early neonatal starvation period, Nature 432 (2004) 1032–1036.
[31] J. Rakar, S. Lonnqvist, P. Sommar, J. Junker, G. Kratz, Interpreted gene expression of human dermal fibroblasts after adipo-, chondro- and osteogenic phenotype shifts, Differentiation 84 (2012) 305–313.
[32] S. Liu, D.B. Stolz, P.L. Sappington, C.A. Macias, M.E. Killeen, J.J. Tenhunen, R.L. Delude, M.P. Fink, HMGB1 is secreted by immunostimulated enterocytes and contributes to cytomix-induced hyperpermeability of Caco-2 monolayers, American journal of physiology, Cell Physiol. 290 (2006) C990–C999.
[33] M. Mancini, M. Sedghinasab, K. Knowlton, A. Tam, D. Hockenbery, B.O. Anderson, Flow cytometric measurement of mitochondrial mass and function: a novel method for assessing chemoresistance, Ann. Surg. Oncol. 5 (1998) 287–295.
[34] J.R. Jangamreddy, M.J. Los, Mitoptosis, a novel mitochondrial death mechanism leading predominantly to activation of autophagy, Hepat. Mon. 12 (2012) e6159.
[35] D.W. Hailey, A.S. Rambold, P. Satpute-Krishnan, K. Mitra, R. Sougrat, P.K. Kim, J. Lippincott-Schwartz, Mitochondria supply membranes for autophagosome biogenesis during starvation, Cell 141 (2010) 656–667.
[36] P. Icard, H. Lincet, A global view of the biochemical pathways involved in the regulation of the metabolism of cancer cells, Biochim. Biophys. Acta 1826 (2012) 423–433.
[37] E. Wirawan, T. Vanden Berghe, S. Lippens, P. Agostinis, P. Vandenabeele, Autophagy: for better or for worse, Cell Res. 22 (2012) 43–61.
[38] L.C. Gomes, L. Scorrano, Mitochondrial morphology in mitophagy and macroautophagy, Biochim. Biophys. Acta 1833 (2013) 205–212.
[39] M. Mitani, T. Yamanishi, Y. Miyazaki, N. Otake, Salinomycin effects on mitochondrial ion translocation and respiration, Antimicrob. Agents Chemother. 9 (1976) 655–660.
[40] J.M. Rodriguez-Vargas, M.J. Ruiz-Magana, C. Ruiz-Ruiz, J. Majuelos-Melguizo, A. Peralta-Leal, M.I. Rodriguez, J.A. Munoz-Gamez, M.R. de Almodovar, E. Siles, A.L. Rivas, M. Jaattela, F.J. Oliver, ROS-induced DNA damage and PARP-1 are required for optimal induction of starvation-induced autophagy, Cell Res. 22 (2012) 1181–1198.
[41] S.W. Tait, D.R. Green, Mitochondria and cell signalling, J. Cell Sci. 125 (2012) 807–815.
[42] E. Bossy-Wetzel, D.D. Newmeyer, D.R. Green, Mitochondrial cytochrome c release in apoptosis occurs upstream of DEVD-specific caspase activation and independently of mitochondrial transmembrane depolarization, EMBO J. 17 (1998) 37–49.
[43] P.F. Li, R. Dietz, R. von Harsdorf, p53 regulates mitochondrial membrane potential through reactive oxygen species and induces cytochrome c-independent apoptosis blocked by Bcl-2, EMBO J. 18 (1999) 6027–6036.
[44] E.D. Michelakis, G. Sutendra, P. Dromparis, L. Webster, A. Haromy, E. Niven, C. Maguire, T.L. Gammer, J.R. Mackey, D. Fulton, B. Abdulkarim, M.S. McMurtry, K.C. Petruk, Metabolic modulation of glioblastoma with dichloroacetate, Sci. Transl. Med. 2 (2010) 31ra34.
[45] S. Bonnet, S.L. Archer, J. Allalunis-Turner, A. Haromy, C. Beaulieu, R. Thompson, C.T. Lee, G.D. Lopaschuk, L. Puttagunta, S. Bonnet, G. Harry, K. Hashimoto, C.J. Porter, M.A. Andrade, B. Thebaud, E.D. Michelakis, A mitochondria–K^+ channel axis is suppressed in cancer and its normalization promotes apoptosis and inhibits cancer growth, Cancer Cell 11 (2007) 37–51.
[46] D. Brusa, E. Migliore, S. Garetto, M. Simone, L. Matera, Immunogenicity of 56 degrees C and UVC-treated prostate cancer is associated with release of HSP70 and HMGB1 from necrotic cells, Prostate 69 (2009) 1343–1352.
[47] D.G. Craig, P. Lee, E.A. Pryde, G.S. Masterton, P.C. Hayes, K.J. Simpson, Circulating apoptotic and necrotic cell death markers in patients with acute liver injury, Liver Int. 31 (2011) 1127–1136.
[48] V.M. Betin, J.D. Lane, Caspase cleavage of Atg4D stimulates GABARAP-L1 processing and triggers mitochondrial targeting and apoptosis, J. Cell Sci. 122 (2009) 2554–2566.
[49] M. Djavaheri-Mergny, M.C. Maiuri, G. Kroemer, Cross talk between apoptosis and autophagy by caspase-mediated cleavage of Beclin 1, Oncogene 29 (2010) 1717–1719.
[50] P. Vandenabeele, W. Declercq, F. Van Herreweghe, T. Vanden Berghe, The role of the kinases RIP1 and RIP3 in TNF-induced necrosis, Sci. Signal. 3 (2010) re4.